Greenland tidewater glacier advanced rapidly during era of Norse Settlement

Danni M. Pearce[1†], James M. Lea[2†], Douglas W.F. Mair[2*], Brice R. Rea[3], J. Edward Schofield[3], Nicholas A. Kamenos[4], Kathryn M. Schoenrock[5], Lukasz Stachnik[6], Bonnie Lewis[4], Iestyn Barr[7], Ruth Mottram[8]

[1] Faculty of Environmental Science and Natural Resource Management, Norwegian University of Life Sciences, Ås, 1430, Norway

[2] School of Environmental Sciences, University of Liverpool, Liverpool, L69 3BX, U.K.

[3] School of Geosciences, University of Aberdeen, Aberdeen, AB24 3UF, UK

[4] School of Geographical and Earth Sciences, University of Glasgow, Glasgow, G12 8QQ, UK

[5] School of Natural Sciences, National University of Ireland, Galway, H91 TK33, Ireland

[6] Institute of Geography and Regional Development, University of Wroclaw, Wroclaw, 51-148 Poland

[7] School of Science and the Environment, Manchester Metropolitan University, Manchester, M15 6BH, UK

[8] Danish Meteorological Institute, Copenhagen, 2100, Denmark

ABSTRACT

Our ability to improve prognostic modelling of the Greenland Ice Sheet relies on understanding the long-term relationships between climate and mass flux (via iceberg calving) from marine-terminating tidewater glaciers (TWGs). Observations of recent TWG behavior are widely available but long-term records of TWG advance are currently lacking. Here we present glacial

geomorphological, sedimentological, archeological and modelling data to reconstruct the ~20 km advance of Kangiata Nunaata Sermia during the first half of the last millennium. The data shows that KNS advanced ~15 km during the 12th and 13th centuries CE at a rate of ~115 ma^{-1}, contemporaneous with regional climate cooling towards the Little Ice Age and comparable to rates of TWG retreat witnessed over the last c. 200 years. Presence of Norse farmsteads, proximal to KNS, demonstrate a resilience to climate change, manifest as a rapidly advancing TWG in a cooling climate. The results place limits on the magnitude of ice margin advance and demonstrates TWG sensitivity to climate cooling, as well as warming. These data combined with our grounding line stability analysis provides a long-term record that validates approaches to numerical modeling aiming to link calving to climate.

INTRODUCTION

Reconstructions of Greenlandic TWGs prior to the observation record are limited in number and overwhelmingly dominated by retreat behavior (e.g., Kjeldsen et al., 2015). Such reconstructions are crucial because ice sheet models require validating over longer timescales than the observational record and should ideally include episodes of both ice margin advance and retreat. This would improve confidence in long-term model validation of ice sheet behavior and subsequent projections in sea level change (Pörtner et al., 2019; Vieli and Nick, 2011; Straneo and Heimbach, 2013; Fahrner et al., 2021).

Kangiata Nunaata Sermia (KNS) is the largest outlet TWG south of Jakobshavn Isbræ on Greenland's west coast. It currently has one of the best constrained records of Holocene ice margin change in Greenland spanning the retreat from its Little Ice Age maximum (LIA); 1761 CE) to present (Lea et al., 2014a;b; Pearce et al., 2018; Young et al., 2021). Evidence of glacial

advances are typically not preserved due to sediment reworking, leaving our understanding of TWG dynamics in Greenland and elsewhere largely unconstrained (Kjeldsen et al., 2015; Larsen et al, 2015). We reconstruct the advance of KNS over the last millennium using a multi-proxy approach supported by novel grounding line stability analysis (Fig.1). The geographic and temporal focus of our study also permits the new opportunity to consider the resilience of Norse farmers in the North Western Settlement.

METHODS

To constrain the pre-LIA maximum advance geometry of KNS, we obtained samples for radiocarbon (^{14}C) dating from sedimentary sequences in Austmannadalen and Qamanaarsuup Sermia valleys adjacent to Kangersuneq fjord (Figs.2; 3 and Supp. Methods). To explore the timing of Norse occupation close to the ice margin, we sampled and dated plant macrofossils (charcoal and seeds) extracted from an anthrosol adjacent to ruin group V15 at Umiivik, a farm located beyond, but proximal to, the LIA maximum. Fieldwork was undertaken in Austmannadalen, Qamanaarsuup Sermia and Umiivik in August and September 2015 and August 2016. Processing of material for AMS ^{14}C dating was undertaken at the University of Aberdeen and dating was performed at the ^{14}CHRONO Centre, Queens University Belfast, and at the Beta Analytic Radiocarbon Dating Laboratory in Florida. To evaluate the relative stability of KNS along Kangersuneq, we apply in a novel manner, a well-established equation for determining whether a grounding line occupies a steady state (Schoof, 2007). Explanation of the geomorphological and archaeological context of all sites is presented within each of the sections that follow. For full details see Supp. Methods.

PRE-LITTLE ICE AGE MAXIMUM GLACIER GEOMETRIES

Geomorphological mapping demonstrates that KNS retreated by ~23 km from its LIA maximum, to its present (2021) position, with its lateral margins mostly confined by steep fjord topography along Kangersuneq (Pearce et al., 2018; Fig.1). Evidence for pre-LIA maximum glacier geometries at KNS are preserved within three adjoining valleys that have not been glaciated during the last millennium allowing us to identify locations to reconstruct the advance of KNS (Pearce et al., 2018).

One location is the ice dammed lake Isvand which formed as KNS retreated from its LIA maximum configuration (Fig.1). As KNS continued to thin and retreat into the 21st century the meltwater drainage direction switched in 2004 from Isvand discharging via Austmannadalen (predominantly to the west) to draining subglacially into Kangersuneq (northwest). The river in Austmannadalen is no longer fed by glacier meltwater, leaving an abandoned river channel fed only by a network of small streams which diminish the capacity to move sediment (Weidick and Citterio, 2011) (Fig.1; Fig. SM1). Where the margin of the KNS glacier was at or inland of its 2004 location during the Holocene (Fig.1), as it advanced it would have dammed Isvand and led to the initiation of glacial meltwater discharge and associated sedimentation through Austmannadalen.

In Austmannadalen, we identified well-preserved overbank deposits of silt and fine sand overlying an organic horizon (Fig. 2, Supplemental Methods, and SMI). The upper surface of this organic horizon yielded a AMS ^{14}C age of 972±43 years BP (UBA-31338; cal. 994-1165 CE [95.4%]; Fig. 3). This is consistent with changes in sedimentation observed elsewhere in Greenland used to reconstruct ice margin change prior to the LIA maximum (e.g., Briner et al., 2010). Our evidence provides an earliest date by which KNS advanced to a similar ice margin

and location to that of 2004 that resulted in damming of Isvand and initiation of meltwater discharge into Austmannadalen River.

As KNS advanced toward its LIA maximum position, it dammed the forefield of the Qamanaarsuup Sermia glacier on its northeastern margin, leading to the formation of an extensive ice-dammed lake where glaciolacustrine sediments accumulated (Fig.1). Following the drainage of this lake (1808–1856 CE) (Lea et al., 2014a) subsequent gullying of these sediments revealed a buried organic horizon interpreted to be the land surface prior to lake damming (see Figs.2C-E and Supp. Methods). AMS ^{14}C dating of a pristine terrestrial macrofossil (*bark* indeterminate sp.) – amongst the most reliable materials available for radiocarbon dating in this environment (cf. Edwards et al. 2008) from the top of this organic horizon, returned an age of 800±29 years BP (UBA-31339; cal. 1181-1278 CE [95.4%]; Fig. 2-3). This provides chronological control for the damming of Qamanaarsuup Sermia ice-dammed lake by KNS, which was last directly observed as holding standing water in 1808 (Lea et al., 2014a; Giesecke, 1910) (Fig.1).

GLACIER ADVANCE DURING REGIONAL COOLING

The geometries and chronologies of KNS reconstructed from Austmannadalen and Qamanaarsuup Sermia demonstrate that it advanced by at least 15 km in the early part of the last millennium at a median rate of ~115 m a^{-1} (Figs. 1, 4 and Fig. SM3), before reaching the LIA maximum configuration in 1761 CE with a total advance of ~20 km (Lea et al., 2014a;b). These reconstructed advance rates are comparable to recent rates of TWG retreat observed across Greenland (e.g., Fahrner et al., 2021).

The period of advance coincides with a reduction in reconstructed summer air temperatures during the 12th century in west Greenland (Von Gunten et al., 2012; Lasher and

Yaxford, 2019), which is superimposed on a longer-term regional cooling indicated by a decline in summer $\delta^{18}O$ from the DYE3 ice core (Vinther et al, 2010; Fig.4). It also coincides with a known period of land-terminating glacier expansion in Greenland (Jomelli et al., 2016) and Baffin Island in the Canadian Arctic (Young et al., 2015).

GLACIER STABILITY

The sequence of continuous glaciolacustine deposition in Qamanaarsuup Sermia (Fig.3) indicates that the ice-dammed lake existed for over 500 years from initial damming (1186-1275 CE) to when it drained after 1808. This constrains the margin of KNS between its LIA maximum and 1808 positions during this time (Fig.4A), indicating that the glacier terminus was relatively stable at this extended position despite periods of warming and cooling (Figs.4B, 4C). To evaluate this assertion, and identify other regions of relative margin stability, we implemented a novel, computationally light application of the grounding line boundary layer theory (Schoof, 2007) (See Supp. Methods). Our approach evaluates the potential for a steady state grounding line being achieved along the fjord; primarily driven by a range of potential ice fluxes provided by balance fluxes derived from modern modelled surface mass balance of the KNS catchment, when the glacier margin is known to have been stable (1980-1995; Lea et al., 2014b; Mottram et al., 2017). Results show a clear match between predicted steady state grounding line positions and observed locations where the calving margin was known to be stable during retreat from the LIA maximum, (~1761), providing confidence in our approach (Fig.1).

Both the position at which KNS begins to dam Qamanaarsuup Sermia, and the position of its LIA maximum, are notable in that they coincide with potential steady state glacier margin locations identified by our analysis (Fig.1). These results imply that when the margin of KNS

was located within this area, between 1230±45 and 1808–1856, the glacier would be capable of maintaining a steady state grounding line even if ice fluxes were lower than contemporary values. This helps to explain how KNS maintained an extended configuration that kept Qamanaarsuup Sermia lake dammed, despite multiple warming and cooling episodes which occurred between the 13th and 19th centuries (Fig.4).

NORSE PRESENCE DURING RAPID GLACIER ADVANCE

Our reconstruction indicates that prior to the LIA maximum, the terminus of KNS approached within 5 km of the Norse farmstead at Umiivik (V15) during the occupation of the Norse Western Settlement (~985-1400 CE; Figs. 1, 3 and Fig.SM4; Schofield et al., 2019). The farm ruins at Umiivik are currently extremely difficult to reach by boat due to dense concentrations of icebergs and mélange in Kangersuneq. Given its location on the eastern margin of the fjord, surrounded by steep and mountainous terrain, the site is also impractical to access over land. If similar conditions prevailed during the 11th–14th centuries, navigation in the fjord, using even the smaller conventional boats known to have been used by the Norse would have been extremely challenging, if not impossible (Crumlin-Pedersen, 2010). Radiocarbon dating of an anthrosol, adjacent to the ruins, returned age estimates within the conventionally accepted timing for Norse settlement across this region (Fig.3 and SM4). The occupation of the Norse farmstead at Umiivik was therefore coeval with the rapid advance of KNS and for at least part of the period where the glacier margin was proximal to it.

Since KNS began to retreat from the LIA maximum, between 1761–1808 CE, iceberg concentrations in Kangersuneq appear to have been similar to present (Lea et al., 2014a). Evidence for this is provided by written accounts, maps and photographs from the 19th and 20th

centuries (Lea et al., 2014a; Giesecke, 1910; Roussell, 1941), as well as aerial photographs and satellite imagery from the 20th and 21st centuries (Lea et al., 2014b, Pearce et al., 2018). This leads us to agree with Roussell's (1941, p16) initial assessment upon visiting Umiivik in 1933 that, *'it must be assumed the conditions [in the fjord] in the Middle Ages were different'*. This archaeological evidence implies lower calving fluxes during the Norse period than currently observed, consistent with glaciological behavior that is conducive to our reconstructed glacier advance.

CONCLUSIONS

Our reconstruction of the rapid advance of KNS during the early part of the last millennium demonstrates that regional atmospheric cooling can drive TWG advance at rates comparable to post-LIA and contemporary retreat observed in Greenland. The analysis of glacier margin stability provides the first real-world demonstration that the commonly applied ice sheet model grounding line parameterization can independently identify stable ice margin locations over multi-decadal to multi-centennial timescales (Fig.1). Lower calving fluxes and associated iceberg concentrations in the fjord during ice margin advance are inferred from the occupation of a Norse farmstead proximal to KNS, in an area that is currently very difficult to access by boat. Together, this supports the counter-intuitive notion that a cooling climate would have allowed the Norse easier access by boat to the inner fjord network of the Western Settlement, when viewed relative to the iceberg dominated conditions that exist following the LIA maximum. Our findings provide insight into the dynamic behavior of Greenlandic TWGs during both periods of advance and retreat, allowing those who aim to model their response to climate change to validate their results against a full range of forcing conditions. Confidence in prognostic

simulations of future changes in TWGs and their contributions to global sea level rise will be improved for models that are able to replicate both the advance and retreat phases of this reconstruction.

ACKNOWLEDGMENTS

Authors would like to thank the GINR for providing logistical support in Nuuk. Martin Blicher, Thomas Juul-Pedersen and Johanne Vad for their research and field assistance. We acknowledge the support of the National Museum of Greenland for permission to undertake excavations near to Norse ruin sites (Permit number 2015/03). Project funding was provided by the Leverhulme Trust Research Project Grant 2014-093 and JML was supported by funding from the Quaternary Research Association, British Society for Geomorphology, and a UKRI Future Leaders Fellowship (MR/S017232/1). DMP would like to dedicate this paper to her father Richard M. Pearce.

FIGURE CAPTIONS

Figure 1. Study area with location of sample sites, ^{14}C dates and the results of the grounding line stability analysis. The dates from the buried land surfaces (black labels) show how these relate to the reconstructed locations of KNS (blue labels). Norse ruin group codes follow Bruun (1917). The reconstructed 992–1160 CE glacier configuration is assumed to be analogous to that of 2004 when Isvand began to drain eastwards below KNS (Weidick and Citterio, 2011). Inset, shows the distribution of Western Settlement ruins in this area including farms, storehouses and shielings. Grounding line stability analysis shown for areas where BedMachine v3 bathymetry is available (grey contour lines) (Morlighem et al., 2017), with relatively less stable locations in blue and

more stable locations in red. Selected known ice fronts from last century are shown (white labels) (Lea et al., 2014b).

Figure 2. A) Soil pit stratigraphy for Austmannadalen (RIVA5). ^{14}C dates are available from the organic units at location A5 with ages given in ^{14}C yr BP with *indicating fraction modern ($F^{14}C$). The ^{14}C dates for A5 were taken on the humic acid fraction of organic sediments. B) Photo shows sample retrieval from soil pit A5 using a monolith tin. C) Qamanaarsuup Sermia ice-dammed lake and stratigraphy related to lake impoundment and sedimentation in Qamanaarsuup Sermia following the early LIA advance of KNS. Stratigraphy where sample UBA-31339 was obtained, from the top contact of the peat and the overlying lacustrine unit. Only a partial stratigraphy is found at this site, for full description see SM2 D) Location map; E) Photograph of site UBA-31339.

Figure 3. A) OxCal multiplot comparing the probability distributions of calibrated ^{14}C dates discussed within the text. Brackets indicate the confidence limits (95.4%) on the dates. The vertical dashed lines depict the conventionally acknowledged dates for the start of *landnám* and the end of occupation (abandonment of the farms likely maximum date for the abandonment of the Western Settlement. B) Table of ^{14}C dates from the region around KNS (see Fig.1 for site locations).

Figure 4. KNS marginal location and climate proxy data for the last millennium. (A) Terminus advance and retreat showing key advance stages (blue dashed lines). Median advance scenario (black line, based upon model; see Fig. SM3) shown with 95.4% uncertainty (grey shading)

accounting for probability distribution of radiocarbon dates and variable fjord geometry. (B) Measured $\delta^{18}O$ of chironomids from Scoop Lake (60.70º N 45.42º W; black dots; Lasher et al., 2019), three point moving average (orange line), and 1σ moving average uncertainty (orange shaded area); (C) Alkenone air temperature reconstruction for Braya Sø, Greenland (von Gunten et al., 2012) (66.99°N 51.03°W), showing sample density (white dots), uncertainty (blue shading), and JJA mean Nuuk air temperature (Vinther et al., 2006) (red line) with 10-year mean (black line). (D) 30 year running mean of DYE3 ice core $\delta^{18}O$ observations (Vinther et al., 2010) and standard deviation (red shading). Black dashed lines on panels B-D show the time period of reconstructed advance indicated on panel A.

REFERENCES CITED

1. Bassis, J.N., and Walker, C.C., 2012, Upper and lower limits on the stability of calving glaciers from the yield strength envelope of ice: Proc. Roy. Soc. A-Math. Phy., 468, 913–931, doi.org/10.1098/rspa.2011.0422.n,
2. Briner, J.P., Stewart, H.A.M., Young, N.E., Philipps, W, and Losee, S., 2010, Using proglacial-threshold lakes to ocnstrian fluctuations of the Jakobshavn Isbræ ice margin, western Greenland, during the Holocene, 29, p. 3861-3874, doi.org/10.1016/j.quascirev.2010.09.005
3. Bruun, D., 1917, Oversigt over Nordboruiner i Godthaab- og Frederikshaab-Distrikter: Meddelelser om Grønland, 56(3), p. 55–147.
4. Crumlin-Pedersen, O., 2010, Archaeology and the sea in Scandinavia and Britain: Maritime Culture of the North Vol. 3. Viking Ship Museum, Roskilde, 184 p.
5. Edwards, K.J., Schofield, J.E., and Mauquoy, D., 2008, High resolution paleoenvironmental and chronological investigations of Norse landnám at Tasiusaq,

Eastern Settlement, Greenland: Quaternary Research, 69, p. 1-15, doi:10.1016/j.yqres.2007.10.010.

6. Fahrner, D., Lea, J.M., Brough, S., Mair, D.W.F, Abermann. J., 2021, Linear response of Greenland's tidewater terminus positions to climate: Journal of Glaciology, 67(262), p. 193-203, doi:10.1017/jog.2021.13.
7. Giesecke, K.L., 1910, Mineralogisches Reisejournal über Grönland 1806-13. Meddelelser om Grønland, 35.
8. Jomelli, V., et al. 2016, Paradoxical cold conditions during the medieval climate anomaly in the Western Arctic: Scientific Reports, 6, 32984, doi.org/10.1038/srep32984.
9. Joughin, I., Smith, B.E., Howat, I.M., Scambos, T., and Moon, T., 2010, Greenland flow variability from ice-sheet-wide velocity mapping: Journal of Glaciology, 56(197), 415-430, doi:10.3189/002214310792447734
10. Katz, N.J., Katz, S.V., and Kipiani, M.G., 1965, Atlas and keys of fruits and seeds occurring in the Quaternary deposits of the USS: Nauka, Moscow, 365pp.
11. Kjeldsen, K.K., et al. 2015, Spatial and temporal distribution of mass loss from the Greenland Ice Sheet since AD 1900: Nature, 528(7582), p. 396 – 400, doi.org/10.1038/nature16183.
12. Larsen, N.K., et al. 2015, The response of the southern Greenland ice sheet to the Holocene thermal maximum: Geology, 43(4), p. 291-294, doi.org/10.1130/G36476.1.
13. Lasher, G.E., and Axford, Y., 2019, Medieval warmth confirmed at the Norse Eastern Settlement in Greenland: Geology, 47(3), p. 267-270, doi.org/10.1130/G45833.1.
14. Lea, J.M., et al. 2014a, Terminus-driven retreat of a major southwest Greenland tidewater glacier during the early 19th century: insights from glacier reconstructions and

numerical modelling: Journal of Glaciology, 60, p. 333-344, doi:10.3189/2014JoG13J163.

15. Lea, J.M., et al. 2014b, Fluctuations of a Greenlandic tidewater glacier driven by changes in atmospheric forcing: observations and modelling of Kangiata Nunaata Sermia, 1859–present. The Cryosphere. 8(6), p. 2031-2045, doi.org/10.5194/tc-8-2031-2014.
16. Morlighem, M., et al. 2017, BedMachine v3: Complete bed topography and ocean bathymetry mapping of Greenland from multibeam echo sounding combined with mass conservation: Geophysical Research Letters, 44(21), p. 11051-11061, doi.org/10.1002/2017GL074954.
17. Mottram, R., Boberg, F., Langen, P.L., Yang, S., Rodehacke, C., Jens, C.H., and Madsen, M.S., 2017, Surface mass balance of the Greenland ice sheet in the regional climate model HIRHAM5: Present state and future prospects: Low Temperature Science, 75, p. 105-115, 10.14943/lowtemsci.75.105.
18. Oxford Radiocarbon Accelerator Unit (ORAU) 2021, OxCal online v4.4. https://c14.arch.ox.ac.uk. Last accessed: 8 August 2021.
19. Pearce, D.M., Mair, D.W., Rea, B.R., Lea, J.M., Schofield, J.E., Kamenos, N., and Schoenrock, K., 2018, The glacial geomorphology of upper Godthåbsfjord (Nuup Kangerlua) in southwest Greenland: Journal of Maps, 14(2), p. 45-55, doi.org/10.1080/17445647.2017.1422447.
20. Pörtner, H.O., Roberts, D., Masson-Delmotte, V., Zhai, P., Tignor, M., Poloczanska, E., Mintenbeck, K., Nicolai, M., Okem, A., and Petzold, J., 2019, IPCC Special Report on the Ocean and Cryosphere in a Changing Climate: IPCC Intergovernmental Panel on Climate Change: Geneva, Switzerland.

21. Reimer, P.J., Brown, T.A., and Reimer, R.W., 2004, Discussion: reporting and calibration of post-bomb 14C data: Radiocarbon, 46(3), p. 1299-1304, doi:10.1017/S0033822200033154.
22. Reimer, P.J., et al., 2020, The IntCal20 Northern Hemisphere radiocarbon age calibration curve (0–55 cal kBP): Radiocarbon, 62(4), p.725-757, doi:10.1017/RDC.2020.41.
23. Roussell, A. 1941, Farms and churches in the mediaeval Norse settlements of Greenland. Meddelelser om Gronland, 89, 354
24. Schofield, J.E., Pearce, D.M., Mair, D.W.F., Rea, B.R., Lea, J.M., Kamenos, N.A., Schoenrock, K.M, Barr, I.D., and Edwards, K.J., 2019, Pushing the limits: palynological investigations at the margin of the Greenland Ice Sheet in the Norse Western Settlement: Environmental Archaeology, doi.org/10.1080/14614103.2019.1677075
25. Schoof, C., 2007, Ice sheet grounding line dynamics: Steady states, stability, and hysteresis: Journal of Geophysical Research: Earth Surface, 112(F3), doi.org/10.1029/2006JF000664.
26. Straneo, F., and Heimbach, P., 2013, North Atlantic warming and the retreat of Greenland's outlet glaciers: Nature, 504, p. 36-43, doi.org/10.1038/nature12854.
27. Stuiver, M., and Reimer, P.J., 1993, Extended 14C data base and revised Calib 3.0 14C age calibration program: Radiocarbon, 35(1), p. 215-230, doi:10.1017/S0033822200013904.
28. Vieli, A., and Nick, F.M., 2011, Understanding and modelling rapid dynamic changes of tidewater outlet glaciers: Issues and implications: Surveys in Geophysics, 32, p. 437-458, doi.org/10.1007/s10712-011-9132-4.
29. Vieli, A., Jania, J., and Kolondra, L., 2002, The retreat of a tidewater glacier:

observations and model calculations on Hansbreen, Spitsbergen: Journal of Glaciology, 48(163), 592-600, doi:10.3189/172756502781831089

30. Vinther, B.M., Andersen, K.K., Jones, P.D., Briffa, K.R., and Cappelen, J., 2006, Extending Greenland temperature records into the late eighteenth century: Journal of Geophysical Research: Atmospheres, 111(D11), doi.org/10.1029/2005JD006810.
31. Vinther, B.M., Jones, P.D., Briffa, K.R., Clausen, H.B., Andersen, K.K., Dahl-Jensen, D., Johnsen, S.J., 2010, Climatic signals in multiple highly resolved stable isotope records from Greenland: Quaternary Science Reviews, 29(3-4), p. 522-538, doi.org/10.1016/j.quascirev.2009.11.002.
32. Von Gunten, L., D'andrea, W.J., Bradley, R.S., and Huang, Y., 2012, Proxy-to-proxy calibration: Increasing the temporal resolution of quantitative climate reconstructions: Scientific Reports, 2, 609, doi.org/10.1038/srep00609.
33. Weidick, A. and Citterio, M., 2011, The ice-dammed lake Isvand, West Greenland, has lost its water: Journal of Glaciology, 57(201), p. 186-188, doi:10.3189/002214311795306600.
34. Young, N.E., Lesnek, A.J., Cuzzone, J.K., Briner, J.P., Badgeley, J.A., Balter-Kennedy, A., Graham, B.L., Cluett, A., Lamp, J.L., Schwarz, R., Tuna, T., Bard, E., Caffee, M.W, Zimmerman, S.R.H., and Schaefer, J.M., 2021, In situ cosmogenic 10Be-14C-26Al measurements form recently deglaciated bedrock as a new tool to decipher changes in Greenland Ice Sheet size: Climate of the Past, 17, p. 419-450, doi.org/10.5194/cp-17-419-2021
35. Young, N.E., Schweinsberg, A.D., Briner, J.P., and Schaefer, J.M., 2015, Glacier maxima in Baffin Bay during the Medieval Warm Period coeval with Norse settlement: Science

Advances, 1(11), doi: 10.1126/sciadv.1500806.

FIGURES

Figure 1:

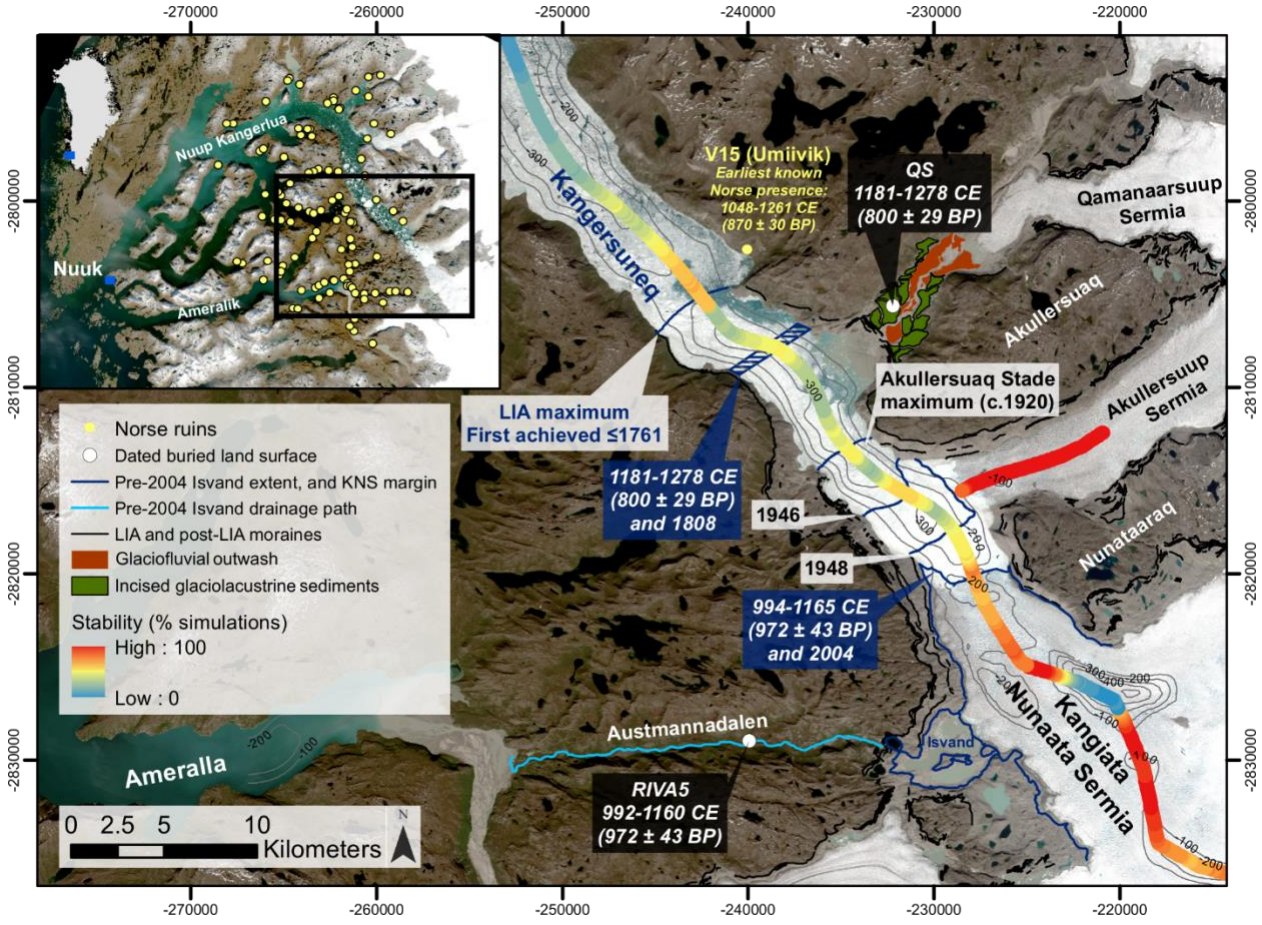

Figure 2:

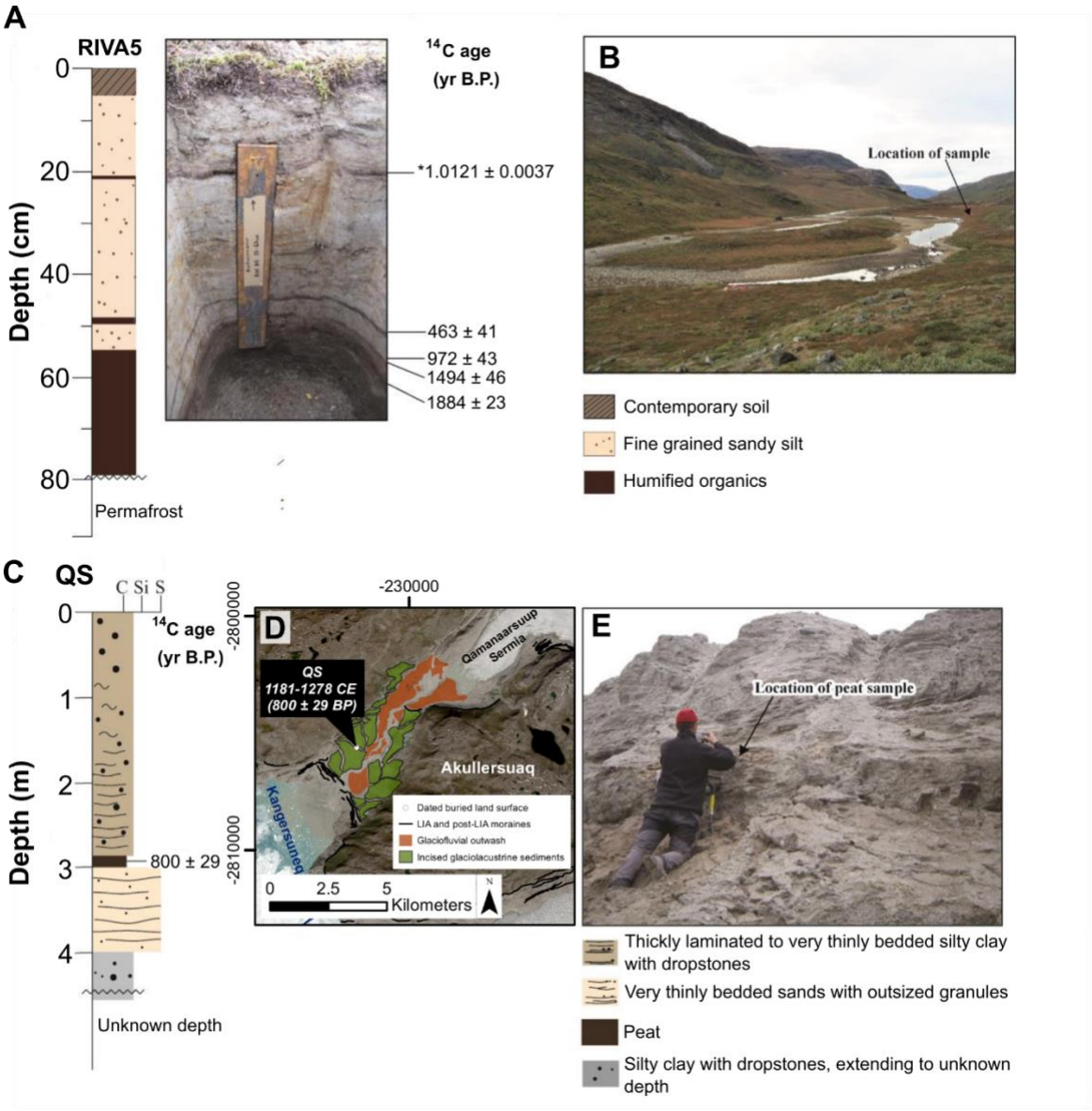
A
RIVA5
Depth (cm)
0
20
40
60
80
Permafrost
14C age
(yr B.P.)
*1.0121 ± 0.0037
463 ± 41
972 ± 43
1494 ± 46
1884 ± 23
B
Location of sample
Contemporary soil
Fine grained sandy silt
Humified organics
C
QS
C Si S
Depth (m)
0
1
2
3
4
800 ± 29
Unknown depth
14C age
(yr B.P.)
-230000
-2800000
-2810000
D
QS
1181-1278 CE
(800 ± 29 BP)
Qamanaarsuup Sermia
Akullersuaq
Kangersuneq
Dated buried land surface
LIA and post-LIA moraines
Glaciofluvial outwash
Incised glaciolacustrine sediments
0 2.5 5
Kilometers
N
E
Location of peat sample
Thickly laminated to very thinly bedded silty clay with dropstones
Very thinly bedded sands with outsized granules
Peat
Silty clay with dropstones, extending to unknown depth

362 Figure 3:

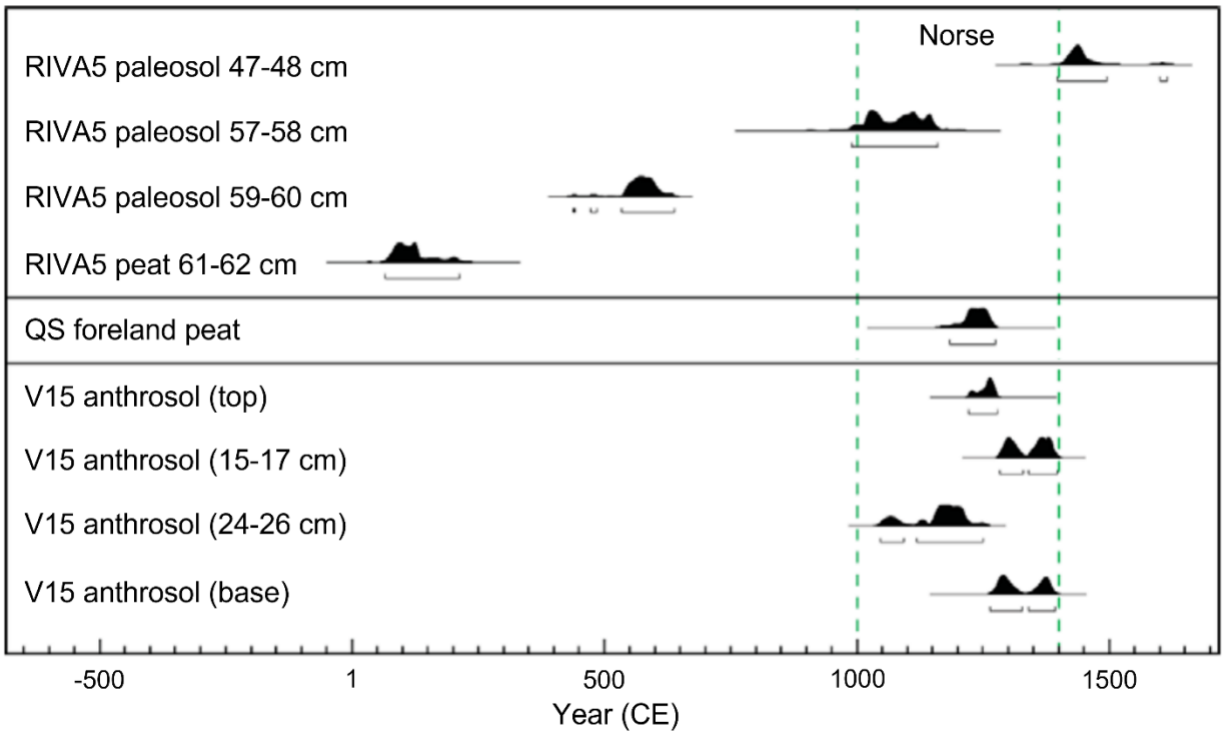

363

364

365 Figure 4:

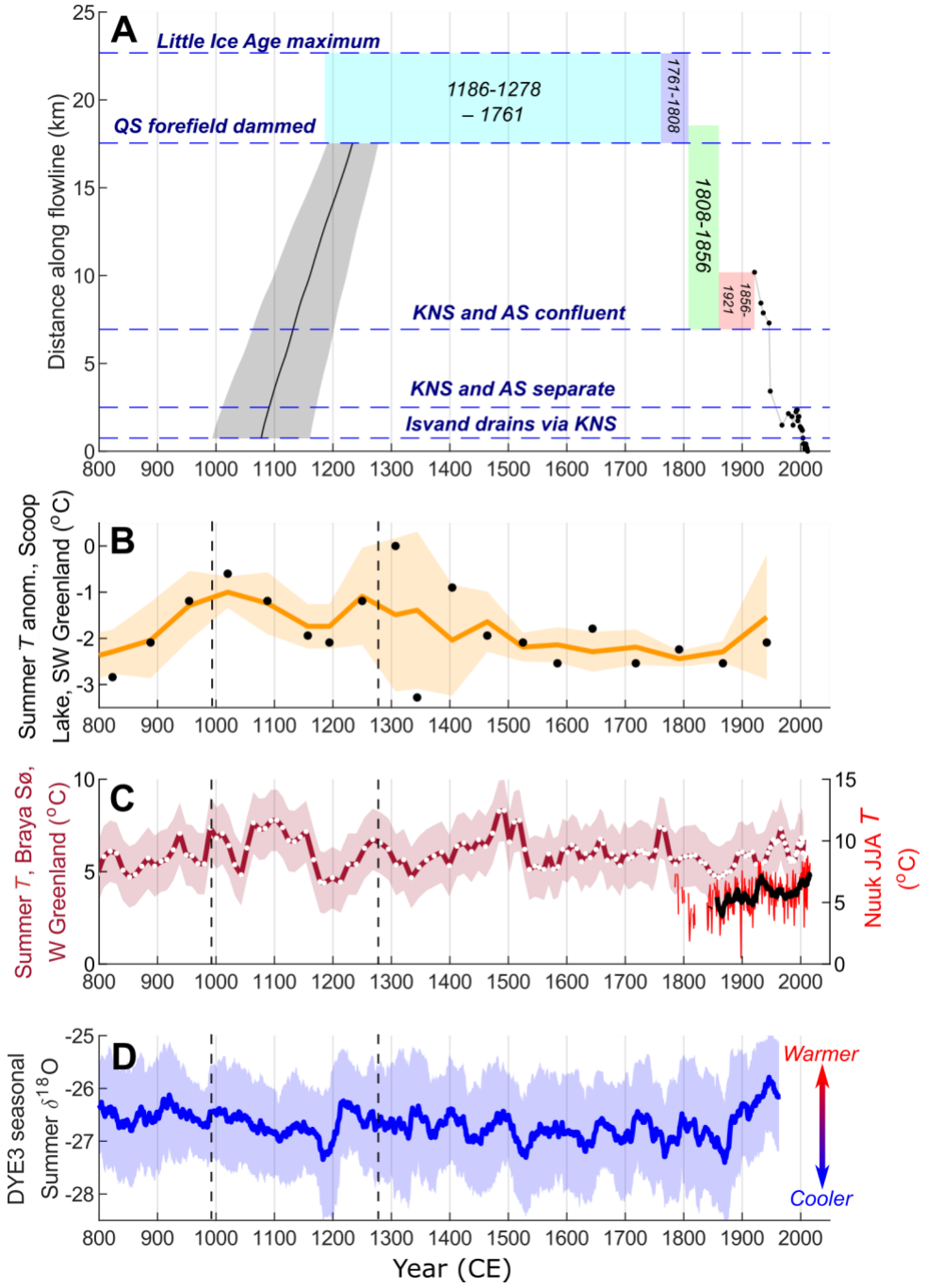
A
Little Ice Age maximum
1186-1278
– 1761
1761-1808
1808-1856
1856-1921
QS forefield dammed
KNS and AS confluent
KNS and AS separate
Isvand drains via KNS
Distance along flowline (km)
B
Summer T anom., Scoop Lake, SW Greenland (°C)
C
Summer T, Braya Sø, W Greenland (°C)
Nuuk JJA T (°C)
D
DYE3 seasonal Summer δ18O
Warmer
Cooler
Year (CE)

366